

SpeakingFaces: A Large-Scale Multimodal Dataset of Voice Commands with Visual and Thermal Video Streams

Madina Abdrakhmanova
ISSAI, Nazarbayev University
Nur-Sultan, Kazakhstan
madina.abdrakhmanova@nu.edu.kz

Askat Kuzdeuov
ISSAI, Nazarbayev University
Nur-Sultan, Kazakhstan
askat.kuzdeuov@nu.edu.kz

Sheikh Jarju
ISSAI, Nazarbayev University
Nur-Sultan, Kazakhstan
sheikh.jarju@nu.edu.kz

Yerbolat Khassanov
ISSAI, Nazarbayev University
Nur-Sultan, Kazakhstan
yerbolat.khassanov@nu.edu.kz

Michael Lewis
ISSAI, Nazarbayev University
Nur-Sultan, Kazakhstan
mlewis@nu.edu.kz

Huseyin Atakan Varol*
ISSAI, Nazarbayev University
Nur-Sultan, Kazakhstan
ahvarol@nu.edu.kz

ABSTRACT

We present SpeakingFaces as a publicly-available large-scale dataset developed to support multimodal machine learning research in contexts that utilize a combination of thermal, visual, and audio data streams; examples include human-computer interaction (HCI), biometric authentication, recognition systems, domain transfer, and speech recognition. SpeakingFaces is comprised of well-aligned high-resolution thermal and visual spectra image streams of fully-framed faces synchronized with audio recordings of each subject speaking approximately 100 imperative phrases. Data were collected from 142 subjects, yielding over 13,000 instances of synchronized data (~3.8 TB). For technical validation, we demonstrate two baseline examples. The first baseline shows classification by gender, utilizing different combinations of the three data streams in both clean and noisy environments. The second example consists of thermal-to-visual facial image translation, as an instance of domain transfer.

CCS CONCEPTS

• **Information systems** → **Multimedia databases**; • **Human-centered computing** → *Human computer interaction (HCI)*; • **Computing methodologies** → *Biometrics*; *Computer vision tasks*.

KEYWORDS

Datasets, Multimodal Learning, Computer Vision, Thermal Imaging, Human-computer Interaction

1 INTRODUCTION

The recent introduction of high-resolution thermal cameras enables new opportunities for multimodal data use in a wide range of applications, such as human-computer interaction (HCI), biometric authentication, recognition systems, domain transfer, and speech recognition. Examples of use-cases with immediate utility include localization of people in circumstances of disaster or in dangerous industrial settings, transit hub surveillance in obscured conditions, and illness detection and contact tracing in public places, an example illustrated by the COVID-19 epidemic [17, 29]. To facilitate such research, we introduce SpeakingFaces, a large-scale dataset consisting of spatially aligned thermal and visual image sequences accompanied by voice command recordings.

*Corresponding author.

High-resolution thermal cameras allow a granular association of temperature values with facial features. The combination of the visual and thermal data can help to overcome the respective drawbacks of each stream [12]. Voice is another important information source for HCI and biometric authentication. The fusion of visual, thermal, and audio data sources opens up new opportunities for research in HCI, and more nuanced analysis of speech in applications, such as the dictation of instructions to smart devices in sub-optimal physical environments, resolution of multi-talker overlapping speech (to distinguish individual speakers and respective intentionality), and improving the performance of automated speech recognition [1].

To date, there have been no datasets that combine all the three data streams, consisting of synchronized visible-spectrum images, thermal images, and audio tracks. Most of the existing thermal-visual facial datasets are constrained by the issues of a small number of subjects, too few unique instances (thus inhibiting data-hungry machine learning algorithms), low resolution of thermal images, or a lack of alignment. These datasets are summarized in Table 1.

The Carl [11] and VIS-TH [22] databases have the fewest image pairs and the lowest resolution of thermal camera, although the latter involved two sessions of each person with four head postures. While the IRIS [16] dataset has the smallest number of subjects, they captured each face from 11 angles. The USTC-NVIE dataset [27] is comprised of the largest number of subjects, but the data were collected using a low-resolution camera.

Table 1: Publicly available datasets where visual and thermal images were acquired simultaneously

Datasets	# Subjects	# Image pairs	Thermal resolution	# Poses	# Trials	Aligned
Carl [11]	41	2,460	160 × 120	1	1	no
IRIS [16]	30	4,228	320 × 240	11	1	no
USTC-NVIE [27]	215	N/A	320 × 240	1	1	no
VIS-TH [22]	50	2,100	160 × 120	4	2	yes
SpeakingFaces	142	4,581,595	464 × 348	9	2	yes

The popular audio-visual datasets include Grid [10], the Oxford-BBC Lip Reading in the Wild (LRW) [9] and the Oxford-BBC Lip Reading Sentences (LRS) [8]. The Grid dataset consists of 34 subjects, each uttering 1,000 sentences. Each sentence has the same structure: verb (4 types) + color (4 types) + preposition (4 types) + alphabet (25 types) + digit (10 types) + adverb (4 types). The main shortcomings are that data acquisition was conducted in a controlled lab environment, and the utterances are unnatural due to the restricted structure of the sentences.

The LRW dataset has a much greater variety in vocabulary and subjects. It is comprised of over one thousand different speakers and up to 400,000 utterances. However, each utterance is an isolated word, 500 unique instances in total, selected from the BBC television. This constraint was addressed in LRS, a large-scale dataset (100,000 natural sentences and a vocabulary size of around 17,000 words), designed to enable lip reading in an unconstrained natural environment. Nevertheless, both LRW and LRS do not contain thermal data.

SpeakingFaces is designed to overcome the limitations of existing datasets. SpeakingFaces consists of 142 subjects, gender-balanced and ethnically diverse. Each subject is recorded in close proximity from nine different angles speaking approximately 100 English phrases or imperative commands, yielding over 13,000 instances of spoken commands, and more than 45 hours of video sequences (over 3.7 million image pairs). The spoken phrases are taken from the Stanford University open source digital assistant database [7], along with publicly available command sets for the Siri virtual assistant [25, 26], chosen to reflect the likely use-case of humans interacting with machines.

The SpeakingFaces dataset can be used in a wide range of multi-modal machine learning contexts, especially those related to HCI, biometrics, and recognition systems. In this work, we demonstrate two baselines: a classifier for gender using all three data streams, and an instance of thermal-to-visual image translation as an example of domain transfer.

2 DATASET DESCRIPTION

In this section, we provide details on the data collection setup and protocol, the data preparation procedure and the database structure. For sessions that involved uttering commands, the preparation of acquired data begins with extracting synchronized video-audio segments. All video segments, from both sessions, are then converted into image sequences. Next, the visual images are aligned with their thermal pairs using heated ArUco markers [13].

2.1 Data Acquisition

The project was conducted with the explicit approval of the Institutional Research Ethics Committee (IREC) of Nazarbayev University. Each subject participated voluntarily and was informed of the data collection and use protocols, including the acquisition of identifiable images which will be shared as a dataset. The informed consent forms were signed by each subject.

The setup for the data collection process is shown in Fig. 1. Subjects were seated in front of the data collection setup at a distance of approximately one meter. The room temperature was regulated at 25 °C. The setup consisted of a metal-framed grid to facilitate



Figure 1: Data acquisition setup for SpeakingFaces.

camera orientation and two 85" video screens upon which textual phrases were simultaneously presented; two screens were used to minimize the need for subjects to turn their heads while reading the phrases.

The video setup consisted of a FLIR T540 thermal camera (resolution 464×348 , wave band $7.5 \mu\text{m} - 14 \mu\text{m}$, and 24° field of view) with an attached visual spectrum camera, a Logitech C920 Pro HD web-camera (resolution 1920×1080 and field of view 78°) that has a built-in dual stereo microphone (44.1 kHz). The web-camera was attached on top of the thermal camera to facilitate subsequent alignment of the image pairs. The original resolution of the web-camera was decreased to 768×512 in order to maximize and align the frame rates for both cameras, while preserving the region-of-interest (RoI), that is the face.

The camera operator proceeded manually through a series of nine positions, as shown in Fig. 2, for approximately 32 seconds of data collection from each position, yielding on average 4.5 minutes of total video per subject. The manual process was consciously chosen over the use of fixed positions (e.g. tripods or mounting frames) so as to introduce small variability in framing and thereby improve the robustness of subsequent machine learning applications. Fig. 2 presents the image pairs from nine predefined positions of nine different subjects.

During the data collection process, the subject sat on a chair as shown in Fig. 1. The height of the chair was adjusted in order to position the top of the subject's head at a predefined mark; in this way, the camera angles did not change significantly from one subject to another. Due to variability in sizes among the participants, the operator manually adjusted the distance from the metal frame, so that the whole face with shoulders was captured, yielding the maximum possible number of pixels per position. Similarly, the operator oriented the side, top and bottom shots to ensure that all of the facial landmarks were fully framed.

Each subject participated in two types of sessions during a single trial. In the first session, subjects were asked to be silent and still, with the operator capturing visual and thermal video streams through the procession of nine collection angles. The second session consisted of the subject reading a series of commands presented one-by-one on the video screens, as visual, thermal and audio data were being collected from the same nine camera positions.

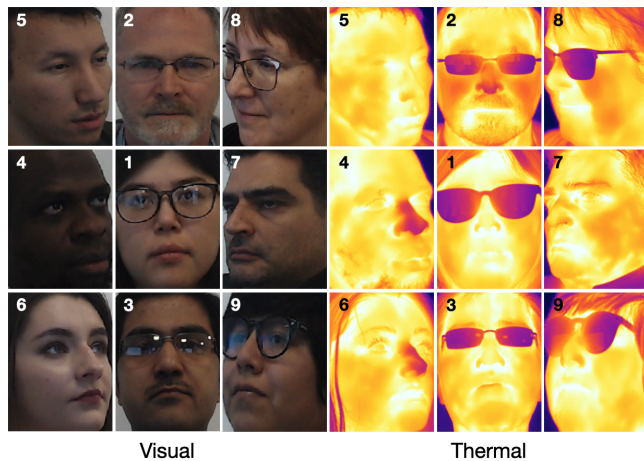


Figure 2: The pairs of visual and thermal facial images of nine subjects taken from the predefined nine positions.

Each subject participated in two trials, conducted on different days, at least two weeks apart, consisting of both types of sessions. This was done in order to account for the day-to-day variations of the subjects. For example, some subjects were wearing glasses during one session and not wearing them in the other. Some subjects changed their hairstyle in between the sessions. Thus, for each subject there are two trials with three data streams (audio, visible-spectrum video, and thermal-spectrum video) and two trials with two data streams (visual and thermal).

The commands were sourced from Thingpedia, an open and crowd-sourced knowledge base for virtual assistants [7]. Thingpedia is a part of the Almond project at Stanford University, and currently includes natural language interfaces for over 128 devices. The interfaces are comprised of utterances grouped by different command types. We selected those that correspond to action and query commands for each device. This resulted in nearly 1,500 unique utterances: 1,297 of them were set aside for training, while the rest were used for test and validation. The total count for the latter part (test and validation) was increased to 500 by utilizing publicly available commands for Siri [25, 26]. We split them in half, such that the commands from Thingpedia would appear evenly in the test and validation sets.

To ensure that each command is uttered by multiple speakers with varying accent, gender, and ethnicity, we reshuffled each of the three sets eight times, as it had been done for the LRW dataset. This approach provided data volumes sufficient for 142 subjects.

2.2 Data Preprocessing

The duration of data collection from each position was set to 900 frames, which, given the data collection rate of 28 frames per second for both cameras, is equivalent to approximately 32 seconds of video. In trials where a subject sat still, without uttering any commands, the raw videos were converted to sequences of 900 images. In the speaking trials, the raw video and audio files were first partitioned into short segments that correspond to the duration of each command utterance.

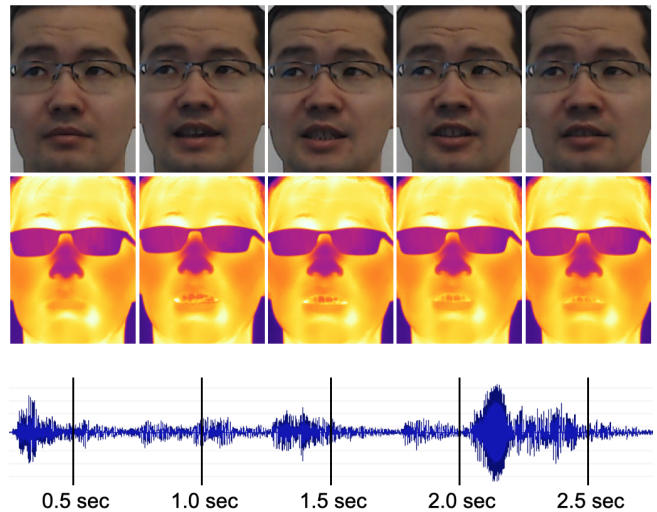


Figure 3: Snapshots from the visual and thermal streams with 0.5-second intervals during the utterance of “stop the kitchen fan from turning”.

The duration for each command utterance was calculated by multiplying the number of characters by the average speed of reading, empirically estimated at 5 frames per character. The commands were partitioned into groups that would maximize the number of utterances within each 900-frame window, based on the utterance duration calculations. The starting and ending frames for each command in a group were annotated, so as to enable the automatic extraction of commands on the basis of the annotations. Fig. 3 shows a sequence of images with 0.5-second intervals illustrating different patterns of the lips during the utterance of a voice command.

Due to the different reading speed among our subjects, the audio segments were manually trimmed leaving at most one second at the end of each utterance. The files were also validated to be complete with minor text noise, such as hesitations or stumbling. The valid recordings were retranscribed to capture the exact utterance in order to further minimize noise in the text data. The video segments were then converted into corresponding image sequences based on the duration of the resulting audio files. Upon the examination of image frames, we have encountered four major artifacts: camera freeze (in thermal), blurriness, flickering, and a slight cut of a chin (in visual). The code for all artifact detection routines can be found in our GitHub repository¹. Blur detection was implemented using the variance of the Laplacian method with OpenCV [4].

Image pairs from the two different cameras were aligned using a method involving the estimation of a planar homography [24]. This process requires matching at least four paired pixel coordinates that correspond to features present in both thermal and visual images. For visual cameras, a printed image of a chessboard is a common calibration object due to its sharp and distinctive features [6]. However, the crispness of the edges degrades significantly when heated and captured by a thermal camera. One way to overcome this issue is to construct a composite chessboard of two different materials [12].

¹<https://github.com/IS2AI/SpeakingFaces>

Another approach utilizes a board with a fixed pattern of holes [18]; when the board is heated, the features become more apparent to a thermal sensor.

For our collection process, we chose ArUco markers, which are synthetic square markers with a black border and a unique binary (black and white) inner matrix that determines its unique identifier (ID) [13]. These markers have been used for robotics [20], autonomous systems [3], and virtual reality [21] thanks to their robustness and versatility. Each detected marker provides the ID and pixel coordinates of its four corners. Detecting these markers in both types of images simplifies the process of obtaining paired pixel coordinates.

We utilized 12 ArUco markers. In order to detect them in a thermal image, the printed copy of the markers was heated using a flood light (Arrilite 750 Plus) and then captured with the setup consisting of thermal and visual cameras. The thermal image was converted to the grayscale and then negated so that the markers would appear similar to the visual image, with black borders and a correctly colored binary matrix. The ArUco detection algorithm successfully found all the 12 markers in both images and generated 48 matched pixel coordinate pairs (12×4) in total. These points were fed to OpenCV’s findHomography function [5] to estimate the homography matrix and warpPerspective function [14] to apply a perspective transformation onto a visual image.

The source code for collecting and pre-processing data is available at our GitHub repository¹ under a BSD license.

2.3 Database Structure

The SpeakingFaces dataset is available through the server of the Institute of Smart Systems and Artificial Intelligence (ISSAI) under Creative Commons Attribution 4.0 International License. ISSAI is a member of DataCite, and a digital object identifier (DOI) was assigned by the ISSAI Repository to the SpeakingFaces dataset².

The database is comprised of 142 subjects in total, with a gender balance of 68 female and 74 male participants, with the ages of participants ranging from 20 to 65, and an average age of 31. Table 2 presents the information on the train/validation/test splits of SpeakingFaces subjects.

The public repository consists of annotated data (metadata), raw data, and clean data. The annotated data include the information on the ID, split (train/valid/test), gender, ethnicity, age, and accessories (hat, glasses, etc.) in both trials for each subject. It also records artifacts detected at each utterance. Depending on the application of the dataset, users can decide which of the artifacts are acceptable and select the data in accordance with their preference. The raw data contain the compressed version of unprocessed video and audio files from both trials for a given subject. The clean data correspond to the result of the whole data preprocessing procedure. Further details on the database structure can be accessed at the repository page³.

3 PRELIMINARY EXPERIMENTS

We developed two baseline tasks to demonstrate the utility and reliability of the SpeakingFaces multimodal dataset. The first task

Table 2: Statistics on SpeakingFaces

Category	Train	Valid	Test	Total
# Speakers	100	20	22	142
Speaker IDs	1-100	101-120	121-142	1-142
# Commands	9,771	1,963	1,977	13,711
# Unique commands	1,297	250	250	1,797
# Tokens	52,769	10,324	11,177	74,270
# Unique tokens	683	337	312	823
# Visual-thermal image pairs for trials with commands	1,054,989	223,528	234,071	1,512,588
# Visual-thermal image pairs for trials w/o commands	1,620,000	356,400	324,000	2,268,000
Duration in hours for trials with commands	16.1	3.2	3.5	22.8
Duration in hours for trials w/o commands	16.1	3.2	3.5	22.8
Size of raw data in TB	5.0	1.0	1.1	7.1

utilizes the three data streams (visual, thermal and audio) to classify the gender of subjects under clean and noisy environments. The second task aims to learn a thermal-to-visual image translation model, to demonstrate a transfer of domain knowledge between the two data streams.

3.1 Gender Classification

The aim of this task is to predict the gender of a subject using the information on a single utterance, consisting of visual, thermal and audio data streams. A successful gender classification approach can improve performance of many applications including human-computer interaction, surveillance and security systems, image/video retrieval, and so on [23].

The gender classification model is based on LipNet [2] architecture consisting of two main modules: an encoder and a classifier. The encoder module is constructed by combining the deep convolutional neural networks (CNN) with the stack of bidirectional recurrent neural network (BRNN) layers ($Encoder(\cdot) \triangleq BRNN(CNN(\cdot))$). This module is used to transform an N -length input feature sequence $X = \{x_1, \dots, x_N\}$ into a hidden feature vector h , that is $h = Encoder(X)$, where x is a three-dimensional tensor for images or a two-dimensional tensor for the spectrograms generated from the audio records. A separate encoder module is trained for each data stream, producing three hidden vector representations: h_{visual} , $h_{thermal}$, and h_{audio} . These generated hidden features are then concatenated and fed to the classifier module.

The classifier module consists of two fully connected layers with the ReLU activation and single linear layer followed by the sigmoid activation ($Classifier(\cdot) \triangleq Sigmoid(Linear(ReLU(ReLU(\cdot))))$), where the linear layer is used to convert a vector to a scalar. The classifier takes the generated hidden features and outputs probability

²<https://doi.org/10.48333/smgd-yj77>

³<https://issai.nu.edu.kz/download-speakingfaces>

Table 3: The accuracy of multimodal gender classification model evaluated on the clean and noisy input data streams

ID	Data streams			Accuracy (%)	
	Visual	Audio	Thermal	Valid	Test
1	clean	clean	clean	89.6	96.0
2			noisy	87.9	95.6
3		noisy	clean	81.9	84.4
4			noisy	76.6	82.0
5	noisy	clean	clean	89.2	93.6
6			noisy	84.5	88.2
7		noisy	clean	67.5	65.8
8			noisy	55.2	50.1

distribution over the two classes $y \in \{female, male\}$, i.e. $P(y|X) = Classifier([h_{visual}^T, h_{thermal}^T, h_{audio}^T]^T)$, where T denotes the transpose operation.

The input feature sequence X is constructed as follows. For visual and thermal streams, we used a sequence of three images extracted from the beginning, middle and end of an utterance. We experimented with the sequence size and observed that three equidistantly spaced images are sufficient to achieve good balance between computational time and performance. For audio streams, we used mel-spectrogram features computed over a 0.4-second snippet extracted from the middle of uttered commands. To evaluate the robustness of multimodal gender classification model, we constructed noisy versions of input features for the validation and test sets. The noisy input features X_{noisy} were generated by adding additive white Gaussian noise (AWGN) $X_{noisy} = X + Z$, where $Z \sim N(0, \Sigma)$. The noise variance Σ for image and audio features was empirically set to 100 and 5, respectively.

All models were trained on a single V100 GPU running on the NVIDIA DGX-2 server using the training set. All hyper-parameters were tuned using the clean validation set. The best-performing model was evaluated using the clean and noisy versions of the validation and test sets.

The model inference results are given in Table 3. In the best-case scenario, when all the three data streams are clean (ID 1), the gender classifier achieves the best accuracy of 96% on the test set. On the other hand, when all the three data streams are noisy (ID 8), the model performance is random, equivalent to a coin toss. In other scenarios, when one or two data streams are corrupted (IDs 2-7), the model achieves an accuracy of 65.8%-95.6% on the test set, which highlights the robustness of multimodal systems. We observed that the most informative data stream is the audio followed by the visual and thermal streams. For example, when the audio stream is corrupted, the accuracy drops by 11.6% (ID 1 vs ID 3), whereas for the visual and the thermal streams the accuracy drops by 2.4% (ID 1 vs ID 5) and 0.4% (ID 1 vs ID 2) respectively. Although the thermal stream is the least effective, it is extremely useful when the visual stream is corrupted (e.g. at night) where 5.4% improvement on the test set is gained (ID 5 vs ID 6). These experimental results successfully demonstrate the advantage of using multiple data streams and the utility of SpeakingFaces dataset.

3.2 Thermal-to-Visual Facial Image Translation

Facial features present in the visible images are not clearly observable in their thermal versions (see Fig. 2). As a result, models (i.e. facial landmark detection, face recognition) developed for visual images cannot be utilized on thermal images. Therefore, in this work, we aim to address the problem of generating a realistic visual-spectrum version of a given thermal facial image.

Generative Adversarial Networks (GANs) [15] have been successfully deployed for generating realistic images; in particular, Pix2Pix [19] and CycleGAN [31] have been shown to produce promising results in translating images from one domain to another. Zhang et al. introduced a Pix2Pix-based approach that focused on achieving a high face recognition accuracy of their generated visible images by incorporating an explicit closed-set face recognition loss [30]. However, their image output lacked the distinct facial features and high image quality which was the priority of Wang et al. [28]. They combined CycleGAN with a new detector network that located facial landmarks in generated visible images and aimed to guide the generator in producing realistic results. Both works suffered from a small number of image pairs and low resolution of thermal cameras. Zhang et al. filtered IRIS dataset [16] down to 695 image pairs and Wang et al. collected 792 image pairs using FLIR AX5 thermal camera with a resolution of 320×256 . The latter dataset is not publicly available.

In our case, we deployed CycleGAN to map thermal faces to visual-spectrum. The generator architecture was set to resnet_9 blocks. For training, we used 8,359 image pairs, coming from the speaking and non-speaking sessions of the train and validation splits (120 subjects). Then, the model was tested on 1,474 “speaking” and “non-speaking” image pairs (22 subjects), and the results are shown in Fig. 4. The generated images are quite realistic; they are close to the target visible images not only in the structure of facial features, but also in overall appearance for a variety of head postures. The model produces smooth and coherent skin texture and color. Also, it learned to correctly predict the gender of each person. For example, the generator drew facial hair for the male subjects. In addition, in some cases the model wears makeup on female subjects (ID 4 and ID 5). Most interestingly, the model learned to generate realistic fake eyes for subjects with glasses (i.e. ID 3 and ID 9). Overall, the hair is realistically drawn, but the model is biased towards brown haired individuals, so it failed to provide the right hair color for subject 1. Also, the model biased towards young people, because 34% of participated subjects were 20-25 years old. As a result, in some cases, the model generates a younger version of a subject (ID 3 and ID 9).

4 CONCLUSION

We introduced SpeakingFaces, a large-scale multimodal dataset designed to encourage research in the general areas of human-computer interaction, biometric authentication, and recognition systems.

SpeakingFaces is designed to overcome constraints in extant relevant datasets which are limited by factors, such as too few subjects, a lack of data instances, low resolution of the source data, and a lack of alignment of the data streams.

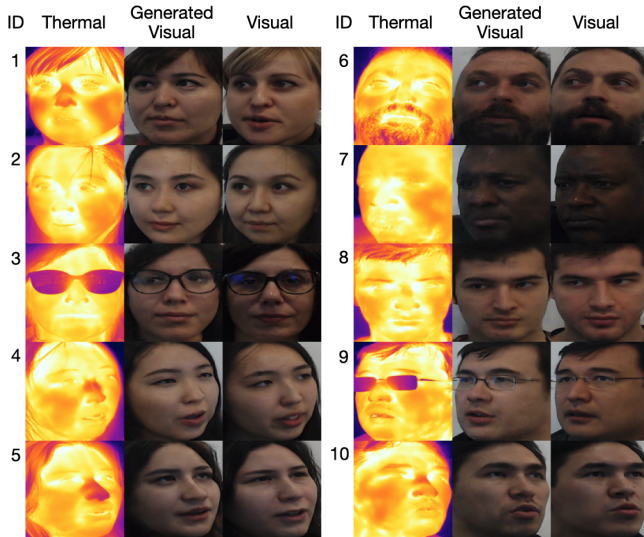


Figure 4: Thermal-to-visual image translation results using CycleGAN. For each column, left to right: real thermal image; generated visual image; and real visual image.

We applied our data to thermal to visible image translation using CycleGAN and also gender classification using thermal, visible and audio data streams. In future work, we plan to utilize our dataset in other multimodal tasks, such as audio-visual-thermal speech recognition and speaker recognition.

REFERENCES

[1] Triantafyllos Afouras, Joon Son Chung, Andrew Senior, Oriol Vinyals, and Andrew Zisserman. 2018. Deep audio-visual speech recognition. *IEEE Transactions on Pattern Analysis and Machine Intelligence* (2018).

[2] Yannis M. Assael, Brendan Shillingford, Shimon Whiteson, and Nando de Freitas. 2016. LipNet: Sentence-level Lipreading. *CoRR* abs/1611.01599 (2016). arXiv:1611.01599 <http://arxiv.org/abs/1611.01599>

[3] Jan Bacik, Frantisek Durovsky, Pavol Fedor, and Daniela Perdukova. 2017. Autonomous flying with quadcopter using fuzzy control and ArUco markers. *Intelligent Service Robotics* 10, 3 (2017), 185–194. <https://doi.org/10.1007/s11370-017-0219-8>

[4] Blur detection with OpenCV. Accessed: April 8, 2020. <https://www.pyimagesearch.com/2015/09/07/blur-detection-with-opencv/>.

[5] Camera Calibration and 3D Reconstruction. Accessed: Dec 5, 2019. https://docs.opencv.org/2.4/modules/calib3d/doc/camera_calibration_and_3d_reconstruction.html.

[6] Camera calibration With OpenCV. Accessed: Dec 5, 2019. https://docs.opencv.org/2.4/doc/tutorials/calib3d/camera_calibration/camera_calibration.html.

[7] Giovanni Campagna, Rakesh Ramesh, Silei Xu, Michael Fischer, and Monica S Lam. 2017. Almond: The architecture of an open, crowdsourced, privacy-preserving, programmable virtual assistant. In *Proc. of the International Conference on World Wide Web*. 341–350.

[8] Joon Son Chung, Andrew Senior, Oriol Vinyals, and Andrew Zisserman. 2017. Lip reading sentences in the wild. In *Proc. of the IEEE Conference on Computer Vision and Pattern Recognition (CVPR)*. IEEE, 3444–3453.

[9] J. S. Chung and A. Zisserman. 2016. Lip Reading in the Wild. In *Asian Conference on Computer Vision*.

[10] Martin Cooke, Jon Barker, Stuart Cunningham, and Xu Shao. 2006. An audio-visual corpus for speech perception and automatic speech recognition. *The Journal of the Acoustical Society of America* 120, 5 (2006), 2421–2424.

[11] Virginia Espinosa-Duró, Marcos Faundez-Zanuy, and Jiri Mekyska. 2013. A New Face Database Simultaneously Acquired in Visible, Near-Infrared and Thermal Spectrums. *Cognitive Computation* 5 (03 2013), 119–135. <https://doi.org/10.1007/s12559-012-9163-2>

[12] Rikke Gade and Thomas B Moeslund. 2014. Thermal cameras and applications: a survey. *Machine Vision and Applications* 25, 1 (2014), 245–262.

[13] Sergio Garrido-Jurado, Rafael Muñoz-Salinas, Francisco José Madrid-Cuevas, and Manuel Jesús Marín-Jiménez. 2014. Automatic generation and detection of highly reliable fiducial markers under occlusion. *Pattern Recognition* 47, 6 (2014), 2280–2292.

[14] Geometric Image Transformations. Accessed: Dec 5, 2019. https://docs.opencv.org/2.4/modules/imgproc/doc/geometric_transformations.html.

[15] Ian Goodfellow, Jean Pouget-Abadie, Mehdi Mirza, Bing Xu, David Warde-Farley, Sherjil Ozair, Aaron Courville, and Yoshua Bengio. 2014. Generative Adversarial Nets. In *Advances in Neural Information Processing Systems*, Z. Ghahramani, M. Welling, C. Cortes, N. D. Lawrence, and K. Q. Weinberger (Eds.). Curran Associates, Inc., 2672–2680. <http://papers.nips.cc/paper/5423-generative-adversarial-nets.pdf>

[16] R. I Hammoud. Accessed: Jan 20, 2020. IEEE OTCBVS WS Series Bench. <http://vcip1-okstate.org/pbvs/bench/>.

[17] Chaolin Huang, Yeming Wang, Xingwang Li, Lili Ren, Jianping Zhao, Yi Hu, Li Zhang, Guohui Fan, Jiuyang Xu, Xiaoying Gu, et al. 2020. Clinical features of patients infected with 2019 novel coronavirus in Wuhan, China. *The Lancet* 395, 10223 (2020), 497–506.

[18] Soonmin Hwang, Jaesik Park, Namil Kim, Yukyung Choi, and In So Kweon. 2015. Multispectral pedestrian detection: Benchmark dataset and baseline. In *Proc. of the IEEE Conference on Computer Vision and Pattern Recognition (CVPR)*. 1037–1045.

[19] Phillip Isola, Jun-Yan Zhu, Tinghui Zhou, and Alexei A Efros. 2017. Image-to-image translation with conditional adversarial networks. In *Proc. of the IEEE Conference on Computer Vision and Pattern Recognition (CVPR)*. 1125–1134.

[20] A. Kuzdeuov, M. Rubagotti, and H. A. Varol. 2020. Neural Network Augmented Sensor Fusion for Pose Estimation of Tensegrity Manipulators. *IEEE Sensors Journal* (2020), 1–1. <https://doi.org/10.1109/JSEN.2019.2959574>

[21] R. G. Lupu, P. Herghelegiu, N. Botezatu, A. Moldoveanu, O. Ferche, C. Ilie, and A. Levinta. 2017. Virtual reality system for stroke recovery for upper limbs using ArUco markers. In *Proc. of the International Conference on System Theory, Control and Computing (ICSTCC)*. 548–552. <https://doi.org/10.1109/ICSTCC.2017.8107092>

[22] Khawla Mallat and Jean-Luc Dugelay. 2018. A benchmark database of visible and thermal paired face images across multiple variations. In *International Conference of the Biometrics Special Interest Group, BIOSIG 2018, Darmstadt, Germany, September (LNI)*. GI / IEEE, 199 – 206.

[23] Preeti Rai and Pritee Khanna. 2012. Gender classification techniques: A review. In *Advances in Computer Science, Engineering & Applications*. Springer, 51–59.

[24] Richard Szeliski. 2010. *Computer vision: algorithms and applications*. Springer Science & Business Media.

[25] The best Siri commands for iOS and MacOS. Accessed: Dec 20, 2019. <https://www.digitaltrends.com/mobile/best-siri-commands/>.

[26] The complete list of Siri commands. Accessed: Dec 22, 2019. <https://www.cnet.com/how-to/the-complete-list-of-siri-commands/>.

[27] S. Wang, Z. Liu, S. Lv, Y. Lv, G. Wu, P. Peng, F. Chen, and X. Wang. 2010. A Natural Visible and Infrared Facial Expression Database for Expression Recognition and Emotion Inference. *IEEE Transactions on Multimedia* 12, 7 (Nov 2010), 682–691. <https://doi.org/10.1109/TMM.2010.2060716>

[28] Zhongling Wang, Zhenzhong Chen, and Feng Wu. 2018. Thermal to visible facial image translation using generative adversarial networks. *IEEE Signal Processing Letters* 25, 8 (2018), 1161–1165.

[29] World Health Organization. Accessed: March 5, 2020. Novel Coronavirus - China. <https://www.who.int/csr/don/12-january-2020-novel-coronavirus-china/en/>.

[30] Teng Zhang, Arnold Wiliem, Siqi Yang, and Brian Lovell. 2018. Tv-gan: Generative adversarial network based thermal to visible face recognition. In *Proc. of the International Conference on biometrics (ICB)*. 174–181.

[31] Jun-Yan Zhu, Taesung Park, Phillip Isola, and Alexei A Efros. 2017. Unpaired image-to-image translation using cycle-consistent adversarial networks. In *Proc. of the IEEE International Conference on Computer Vision*. 2223–2232.